

Porous Coordination Polymer with Pyridinium Cationic Surface, $[\text{Zn}_2(\text{tpa})_2(\text{cpb})]$

Masakazu Higuchi,[†] Daisuke Tanaka,[‡] Satoshi Horike,[‡] Hirotohi Sakamoto,[‡] Kohei Nakamura,[‡] Yohei Takashima,[‡] Yuh Hijikata,[‡] Nobuhiro Yanai,[‡] Jungeun Kim,[§] Kenichi Kato,[†] Yoshiki Kubota,^{||,†} Masaki Takata,^{†,§} and Susumu Kitagawa^{*,†,‡,⊥}

RIKEN SPring-8 Center, 1-1-1, Kouto, Sayo-cho, Sayo-gun, Hyogo 679-5148, Japan, Department of Synthetic Chemistry & Biological Chemistry, Graduate School of Engineering, Kyoto University, Katsura, Nishikyo-ku, Kyoto 615-8510, Japan, Japan Synchrotron Radiation Research Institute, 1-1-1, Kouto, Sayo-cho, Sayo-gun, Hyogo 679-5198, Japan, Department of Physical Science, Graduate School of Science, Osaka Prefecture University, Sakai, Osaka 599-8531, Japan, Institute for Integrated Cell-Material Sciences, Kyoto University, 69 Konoe-cho, Yoshida, Sakyo-ku, Kyoto 606-8501, Japan

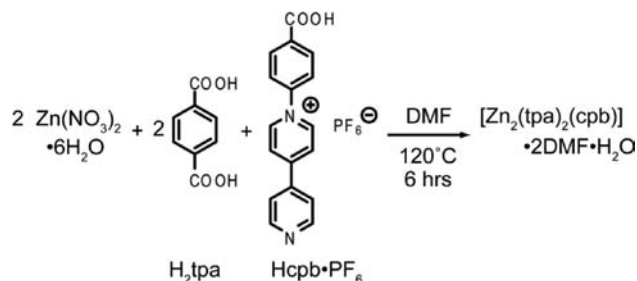
Received January 17, 2009; E-mail: kitagawa@sbchem.kyoto-u.ac.jp

The design and construction of metal–organic crystal architectures have been widely studied, and a variety of frameworks have emerged via self-assembly processes.¹ In particular, there is a growing interest in the study of porous coordination polymers (PCPs) with micropores and well-designed pore surfaces.² Functionalization of pore surfaces is a very attractive idea for applications in gas storage,³ separation,⁴ and catalysis.^{5,6} Porous frameworks in this category can be designed and synthesized by using appropriate ligands, usually stiff aromatic ones having functional sites, i.e., for hydrogen bonding⁷ (functional organic site (FOS)⁶) and electrostatic interaction.⁸ Although utilization of them is relevant for PCPs, the interacting area is usually restricted to narrower sites.

Here we focus on electrostatic interaction sites because we expect a stronger confinement effect than that in the case of dispersion-type interaction. Several charged frameworks have been synthesized.⁹ In these frameworks, the resulting PCPs contain a counteranion or cation in the pore for charge compensation, and therefore, the pores are significantly blocked against guest species. To retain an electrostatic interaction site as a guest-accessible FOS, we designed a charge-separated neutral organic linker, in which a pyridinium cation and a carboxylate act as an FOS and a coordination site, respectively. We report here the synthesis and the methanol sorption property of a PCP with a pyridinium cationic surface. We also estimated the isosteric heat of adsorption for methanol of a polar molecule to elucidate the adsorbate–adsorbent interaction.

The reaction of $\text{Zn}(\text{NO}_3)_2 \cdot 6\text{H}_2\text{O}$ with terephthalic acid (H_2tpa) and 1-(4-carboxyphenyl)-4,4'-bipyridinium hexafluorophosphate¹⁰ ($\text{Hcpb} \cdot \text{PF}_6$) affords the porous coordination polymer, $[\text{Zn}_2(\text{tpa})_2(\text{cpb})] \cdot 2\text{DMF} \cdot \text{H}_2\text{O}$ ($1 \supset 2\text{DMF} \cdot \text{H}_2\text{O}$), in which the cpb ligand acts as a neutral one (Scheme 1). Notably, $1 \supset 2\text{DMF} \cdot \text{H}_2\text{O}$ does not include any counteranion from the starting materials, such as OH^- , NO_3^- , and PF_6^- . The crystal structure of $1 \supset 2\text{DMF} \cdot \text{H}_2\text{O}$ was determined by single-crystal X-ray crystallography at 213 K.¹¹ Figure 1a shows the coordination environment of Zn^{2+} . The asymmetric unit contains two each of Zn^{2+} and tpa^{2-} and one of cpb. The two Zn^{2+} atoms are hepta- and hexacoordinated to four O atoms from each two of the monodentate and bidentate carboxylate groups coming from tpa and to one N atom from the pyridine of cpb, respectively. Figure 1b shows a presentation of the resulting two types of pores surrounded by $[\text{Zn}_2(\text{tpa})_2(\text{cpb})]$; pore A is enclosed by the four tpa ligands and the two bipyridine parts of the cpb ligands, and pore B is between the two benzoate parts of the cpb ligands and the four tpa ligands. Figure

Scheme 1



1c illustrates a view of the 3D structure of $1 \supset 2\text{DMF} \cdot \text{H}_2\text{O}$ built of an interpenetrated 2D porous framework (green and pink colors). The π – π stacking interaction between the tpa ligand and the pyridinium part of the cpb ligand allows for the construction of these 3D structures. Compound $1 \supset 2\text{DMF} \cdot \text{H}_2\text{O}$ possesses straight 2D channels along (101) and (010) directions with cross sections of $2.7 \times 4.9 \text{ \AA}^2$ and $6.0 \times 12.1 \text{ \AA}^2$, respectively. The pyridinium part of the cpb ligand is exposed to the pore surface. The total void volume, V_{void} , is 36.3% per unit volume as determined by PLATON.¹² Thermogravimetric analysis (TGA) performed on $1 \supset 2\text{DMF} \cdot \text{H}_2\text{O}$ shows a weight loss of 18.9% from 298 to 423 K (Figure S1). This corresponds to the loss of two DMFs and one H_2O per formula unit (calcd 18.3%), which is supported by the result of elemental analysis. No further weight loss steps were

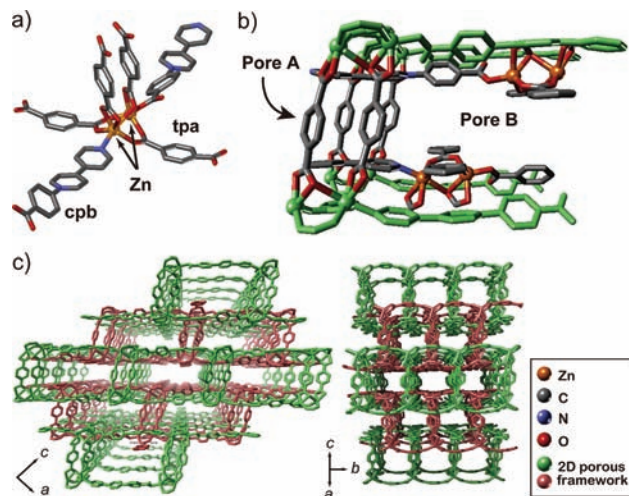


Figure 1. (a) Crystallographic environment around Zn(II) dimer. (b) Pore surface composed of $2[\text{Zn}_2(\text{tpa})_2(\text{cpb})]$. (c) Three dimensional assembled structure of $1 \supset 2\text{DMF} \cdot \text{H}_2\text{O}$. Hydrogen atoms and guests in the pore are omitted for clarity.

[†] RIKEN Spring-8 center

[‡] Department of Synthetic Chemistry & Biological Chemistry, Kyoto University.

[§] Japan Synchrotron Radiation Research Institute.

^{||} Osaka Prefecture University.

[⊥] Institute for Integrated Cell-Material Sciences, Kyoto University.

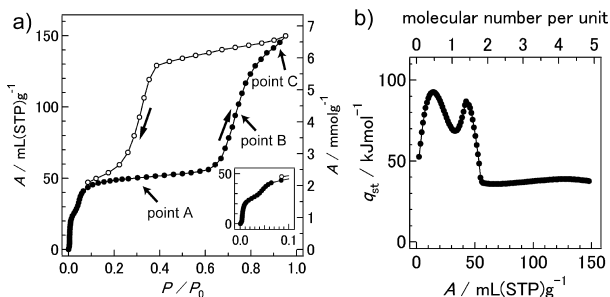


Figure 2. (a) Sorption isotherms of methanol at 297.39 K for **1**. XRPD patterns at points A–C were obtained. Inset shows low pressure region. (b) Isothermic heat of adsorption, q_{st} , of methanol on **1** plotted against the amount of adsorption.

observed below 623 K after removal of the guests. This indicates the heat stability of **1** up to 523 K. The flexibility of the framework was also confirmed by X-ray powder diffraction (XRPD) measurement (Figure S2b and c).¹³

After degassing treatment of $1 \cdot 2\text{DMF} \cdot \text{H}_2\text{O}$ at 423 K for 12 h in vacuo, the nitrogen sorption isotherm at 77 K for **1** shows the permanent porosity (Figure S3). To examine the surface potential, the methanol sorption isotherms for **1** at 298 K were measured, as shown in Figure 2 and S4. A saturated adsorbed amount of ca. $150 \text{ mL} \cdot \text{g}^{-1}$ corresponds to five methanol molecules per unit, $[\text{Zn}_2(\text{tpa})_2(\text{cpb})]$. The adsorption isotherm of methanol undergoes slight and distinct steps at $P/P_0 = 0.03$ and 0.6 , respectively, accompanied with sorption hysteresis, indicating a structural transformation induced by methanol inclusion¹⁷ (see below). The first, second, and third uptake correspond to one, one, and three methanol molecules per unit sorption. To elucidate the adsorbate–adsorbent interaction, the isosteric heat of adsorption q_{st} was calculated as a function of the adsorption amount (Figure 2b), employing the virial-type equation in conjunction with the three temperature isotherms.¹¹ The q_{st} value for the initial two methanol molecules per unit gave values in the range $50\text{--}95 \text{ kJ mol}^{-1}$ with two maxima, whereas that for subsequent adsorption was fixed at $\sim 40 \text{ kJ mol}^{-1}$. To date, the q_{st} value is found to be below 55 kJ mol^{-1} , even though the effects of the methanol–methanol interaction, hydrogen bond between the methanol framework, the accessible metal site, and an adsorption in microporosity were included.¹⁴ Despite the absence of an accessible metal site in **1**, the incipient q_{st} values of $50\text{--}95 \text{ kJ mol}^{-1}$, therefore, were significantly large and are comparable to those of alkali metal exchanged molecular sieves, in the range $90\text{--}100 \text{ kJ mol}^{-1}$.¹⁵ On the other hand, the values obtained for the subsequent adsorption of 40 kJ mol^{-1} compare with the vaporization enthalpy of methanol, 37.4 kJ mol^{-1} .¹⁶ This indicates that there is no specific surface left after the adsorption of the initial two methanol molecules per unit. These results imply that the pyridinium cationic surface is involved in the initial strong adsorption of methanol. To investigate any structural transformation during the methanol adsorption, the XRPD pattern was measured at points A ($P/P_0 = 0.3$), B (0.7), and C (0.9) as shown in Figure 2a. The whole-powder-pattern fitting by the Le Bail method reveals that the early two and three methanol inclusions induce the shrinkage ($V = 7649(1) \text{ \AA}^3$) and expansion ($8263(2) \text{ \AA}^3$) of the 2D porous layers from the framework of the as-synthesized $1 \cdot 2\text{DMF} \cdot \text{H}_2\text{O}$ ($8048(1) \text{ \AA}^3$), respectively. This change in cell volume is mainly involved in shrinkage and expansion of the c axis, as evident from the shifts of the index peak 002 in Figure S2d–f and Table S1. This framework transformation of **1** presumably will also enable them to adsorb methanol specifically.¹⁷

In summary, we have synthesized a porous coordination polymer containing a pyridinium cation as an organic linker and have investigated the absorptive ability of methanol. Our analysis revealed

that **1** adsorbs methanol with a large isosteric heat of adsorption ($50\text{--}95 \text{ kJ mol}^{-1}$) compared to those of alkali metal exchanged molecular sieves. This result implies that the pyridinium cationic surface participates in the strong adsorption of methanol. Our future work will focus on how guests interact with the aromatic cationic surface. These investigations are in progress.

Acknowledgment. The synchrotron radiation experiments were performed at the BL02B2 and BL44B2 in the SPring-8 with the approval of the Japan Synchrotron Radiation Research Institute (JASRI) and RIKEN (Proposal Nos. 2008A1569 and 20090066, respectively). This work was supported by Nippon Oil Corporation in Japan and by ERATO “Kitagawa Integrated Pore Project” of Japan Science and Technology Agency (JST).

Supporting Information Available: Synthesis, crystallographic data, TGA curve, XRPD patterns for $1 \cdot \text{guests}$, nitrogen isotherm, lattice parameters by Le Bail method, and virial analysis. This material is available free of charge via the Internet at <http://pubs.acs.org>.

References

- (1) (a) Moulton, B.; Zaworotko, M. J. *Chem. Rev.* **2001**, *101*, 1629–1658. (b) Kitagawa, S.; Kitaura, R.; Noro, S. *Angew. Chem., Int. Ed.* **2004**, *43*, 2334–2375. (c) Yaghi, O. M.; O’Keeffe, M.; Ockwig, N. W.; Chae, H. K.; Eddaoudi, M.; Kim, J. *Nature* **2003**, *423*, 705–714.
- (2) (a) Kitagawa, S.; Noro, S.; Nakamura, T. *Chem. Commun.* **2006**, 701–707. (b) Higuchi, M.; Horike, S.; Kitagawa, S. *Supramol. Chem.* **2007**, *19*, 75–78.
- (3) (a) Kondo, M.; Yoshitomi, T.; Seki, K.; Matsuzaka, H.; Kitagawa, S. *Angew. Chem., Int. Ed.* **1997**, *36*, 1725–1727. (b) Frey, G.; Mellot-Draznieks, C.; Serre, C.; Millange, F.; Dutour, J.; Surlbe, S.; Margiolaki, I. *Science* **2005**, *309*, 2040–2042. (c) Rowsell, J. L. C.; Yaghi, O. M. *Angew. Chem., Int. Ed.* **2005**, *44*, 4670–4679.
- (4) (a) Yaghi, O. M.; Li, G. M.; Li, H. L. *Nature* **1995**, *378*, 703–706. (b) Chen, B. L.; Liang, C. D.; Yang, J.; Contreras, D. S.; Clancy, Y. L.; Lobkovsky, E. B.; Yaghi, O. M.; Dai, S. *Angew. Chem., Int. Ed.* **2006**, *45*, 1390–1393.
- (5) (a) Fujita, M.; Kwon, Y. J.; Washizu, S.; Ogura, K. *J. Am. Chem. Soc.* **1994**, *116*, 1151–1152. (b) Wu, C. D.; Hu, A.; Zhang, L.; Lin, W. B. *J. Am. Chem. Soc.* **2005**, *127*, 8940–8941. (c) Horike, S.; Dinca, M.; Tamaki, K.; Long, J. R. *J. Am. Chem. Soc.* **2008**, *130*, 5854–5855.
- (6) Hasegawa, S.; Horike, S.; Matsuda, R.; Furukawa, S.; Mochizuki, K.; Kinoshita, Y.; Kitagawa, S. *J. Am. Chem. Soc.* **2007**, *129*, 2607–2614.
- (7) Kitagawa, S.; Uemura, K. *Chem. Soc. Rev.* **2005**, *34*, 109–119.
- (8) Milfort, K. L.; Hupp, J. T. *Inorg. Chem.* **2008**, *47*, 7936–7938.
- (9) (a) Yang, G.; Raptis, R. G. *Chem. Commun.* **2004**, 2058–2059. (b) Liu, S. X.; Xie, L. H.; Gao, B.; Zhang, C. D.; Sun, C. Y.; Li, D. H.; Su, Z. M. *Chem. Commun.* **2005**, 5023–5025. (c) Olenov, A. V.; Baranov, A. I.; Shevelkov, A. V.; Popovkin, B. A. *Eur. J. Inorg. Chem.* **2002**, 547–553. (d) Lin, Z. J.; Wragg, D. S.; Morris, R. E. *Chem. Commun.* **2006**, 2021–2023. (e) Oliver, S.; Kuperman, A.; Lough, A.; Ozin, G. A. *J. Mater. Chem.* **1997**, *7*, 807–812.
- (10) Bongard, D.; Moller, M.; Rao, S. N.; Corr, D.; Walder, L. *Helv. Chim. Acta* **2005**, *88*, 3200–3209.
- (11) See Supporting Information.
- (12) Spek, A. L. *PLATON, A Multipurpose Crystallographic Tool*; Utrecht University: Utrecht, The Netherlands, 2001.
- (13) Kubota, Y.; Takata, M.; Kobayashi, T. C.; Kitagawa, S. *Coord. Chem. Rev.* **2007**, *251*, 2510–2521.
- (14) (a) Pan, L.; Parker, B.; Huang, X. Y.; Olson, D. H.; Lee, J.; Li, J. *J. Am. Chem. Soc.* **2006**, *128*, 4180–4181. (b) Salame, I. I.; Bandoz, T. *J. Ind. Eng. Chem. Res.* **2000**, *39*, 301–306. (c) Xue, D. X.; Lin, Y. Y.; Cheng, X. N.; Chen, X. M. *Cryst. Growth Des.* **2007**, *7*, 1332–1336. (d) Salame, I. I.; Bandoz, T. *J. Langmuir* **2000**, *16*, 5435–5440. (e) Lee, J. Y.; Olson, D. H.; Pan, L.; Emge, T. J.; Li, J. *Adv. Funct. Mater.* **2007**, *17*, 1255–1262.
- (15) (a) Izmailova, S. G.; Karetina, I. V.; Khvoshchev, S. S.; Shubaeva, M. A. *J. Colloid Interface Sci.* **1994**, *165*, 318–324. (b) Avgul, N. N.; Bezus, A. G.; Dzhitig, O. M. In *Molecular Sieve Zeolites*; Flanigen, E. M., Sand, L. B., Eds.; Advances in Chemistry Series 101; American Chemical Society: Washington, DC, 1971; pp 184–192.
- (16) Weast, R. C.; Astle, M. J.; Beyer, W. H. *CRC Handbook of Chemistry and Physics*, 80th ed; CRC Press: Boca Raton, FL, 1999.
- (17) (a) Kitaura, R.; Fujimoto, K.; Noro, S.; Kondo, M.; Kitagawa, S. *Angew. Chem., Int. Ed.* **2002**, *41*, 133–135. (b) Li, D.; Kaneko, K. *Chem. Phys. Lett.* **2001**, *335*, 50–56. (c) Eddaoudi, M.; Li, H. L.; Yaghi, O. M. *J. Am. Chem. Soc.* **2000**, *122*, 1391–1397. (d) Fletcher, A. J.; Cussen, E. J.; Bradshaw, D.; Rosseinsky, M. J.; Thomas, K. M. *J. Am. Chem. Soc.* **2004**, *126*, 9750–9759. (e) Halder, G. J.; Kepert, C. J. *J. Am. Chem. Soc.* **2005**, *127*, 7891–7900.

JA900373V